

## Assessing Reservoir Uncertainty with Stochastic Facies Modeling of a Hydrothermal Medium Enthalpy Reservoir (Upper Jurassic Carbonates of the Southern German Molasse Basin)

Sebastian Dirner and Ulrich Steiner

ERDWERK GmbH, Bonner Platz 1 D-80803 Munich

dirner@erdwerk.com, steiner@erdwerk.com

**Keywords:** Molasse, Malm, carbonate reservoir, facies model, stochastic modeling

### ABSTRACT

The up to 600 m thick Upper Jurassic carbonates (Malm) at the base of the Molasse Basin in Southern Bavaria (Germany) provide favorable conditions for geothermal energy usage. The hot aquifer (up to 165°C) has so far been explored by 46 geothermal wells reaching depths of up to 5.000 m (TVD) with an overall high success rate of 95%. Typically for carbonates the Malm is a complex and heterogeneous geothermal reservoir with considerably varying reservoir properties in exploration relevant scales. Recent studies showed that reservoir potential (yield) is highly dependent on carbonate facies and diagenetic overprint (e.g. dolomitization and karstification). Reservoir characterization on the basis of borehole data (e.g. cuttings, image logs, etc.) and the correlation to seismic data can improve the predictability of the reservoir in areas with sparse or no well data. To forecast reservoir heterogeneity on an exploration scale and to assess uncertainty, a multi scenario geocellular facies model is set. A stochastic modeling approach (MPS) is used to incorporate inputs from seismic and borehole data as well as outcrop analogues. We present a case study in the greater area of Munich (30x33 km model area) which has the highest density of deep geothermal wells in the Eastern Molasse Basin. Multi equiprobable realizations of the model offer the possibility to assess probability and uncertainty of present reservoir facies. The aim is to minimize exploration risks and in the case of a subsequent flow simulation to forecast more (realistic) production scenarios.

### 1. INTRODUCTION

The up to 600 m thick Upper Jurassic carbonates (Malm) at the base of the Molasse Basin in Southern Bavaria (Germany) provide favourable conditions for geothermal energy usage. The hot aquifer (up to 165°C) has so far (2013) been explored by 46 geothermal wells reaching depths of up to 5.000 m (TVD) with an overall high success rate of 95%. The study area (AOI) is the greater area of Munich, see Figure 1. The AOI extends about 30 km (E-W) and 33 km (N-S) and has the highest density of deep geothermal wells in the Eastern Molasse Basin.

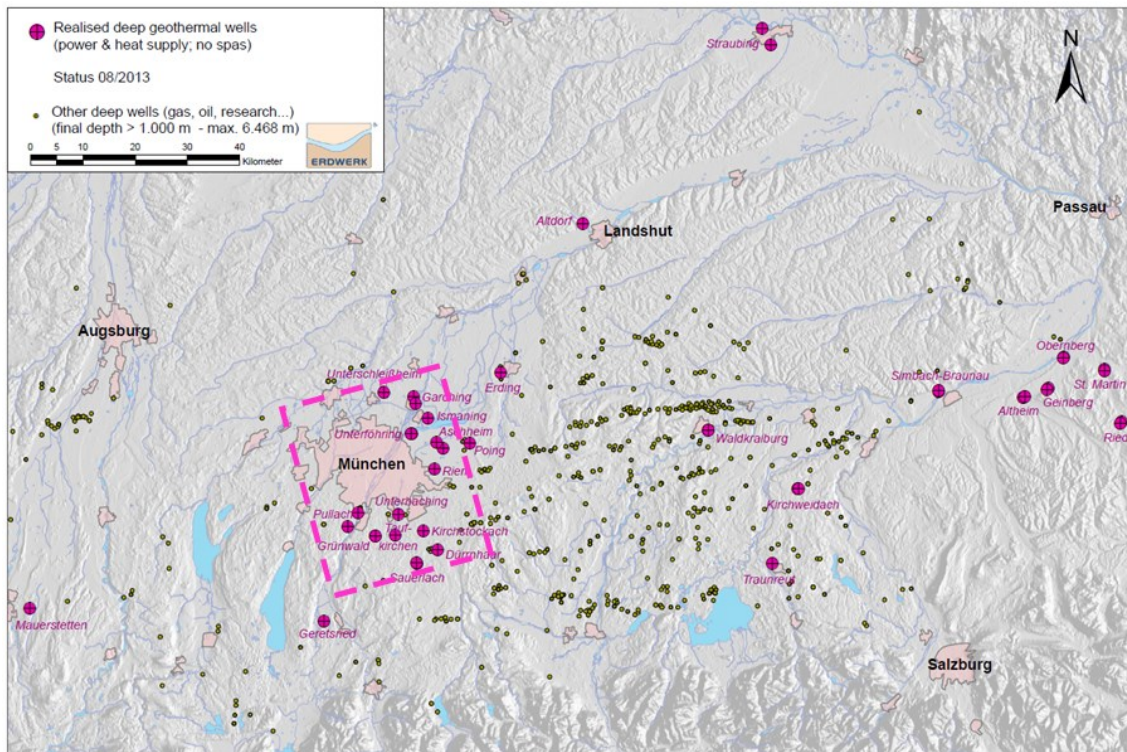


**Figure 1:** Drilled geothermal projects for power and heat supply (pink circles) and other deep oil and gas wells (>1000 m) in the Bavarian Molasse Basin. The pink dashed rectangle outlines the AOI.

## 2. GEOLOGICAL SETTING

The Upper Jurassic Malm carbonates consist of up to 600 m marls and limestones, which can locally be dolomitized. The carbonates crop out in the Swabian and Franconian Alb and dip gently southwards under the North Alpine Foreland Basin, reaching a depth of more than 5.000 m at the boundary to the alpine orogeny, Bachmann, Muller, and Weggen (1987). During the Upper Jurassic, large parts of the European craton were covered with a shelf sea marginal to the oceanic Tethys in the South. In the North, this shelf sea was separated from the boreal sea by an island archipelago. In the southern, deeper part of this epicontinental shelf sea, an extensive siliceous sponge–microbial reef belt developed. According to Meyer and Schmidt-Kaler (1989), the Swabian facies as the central part of this reef belt formed a deeper-water area between the shallower Franconian–Southern Bavarian platform in the East (AOI) and the Swiss platform in the West. To the South, the Swabian facies passed into the Helvetic Basin. The published status quo for the paleogeography of the AOI is ever since the paleogeographic maps from Meyer and Schmidt-Kaler (1989), see Figure 7. The AOI (red circle) in Figure 2 is located on the southern Bavarian reef platform.

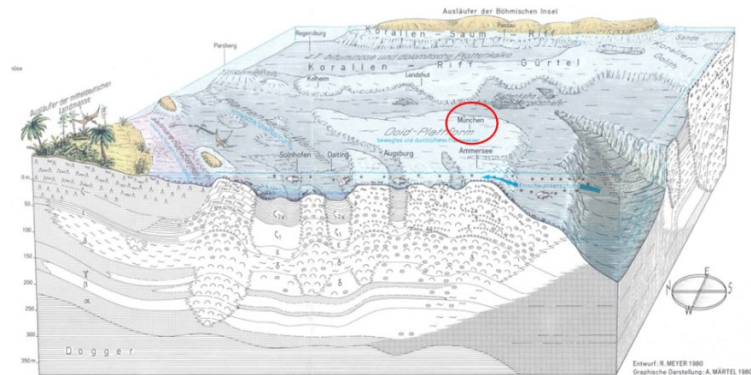


**Figure 2: Palaogeography of the Franconian-Southern Bavarian platform during the Upper Jurassic. The red circle marks the AOI.**

### 3. METHODS AND DATA

Typically for carbonates the Malm is a complex and heterogeneous geothermal reservoir with considerably varying reservoir properties in exploration relevant scales. Recent studies showed that reservoir potential (yield) is highly dependent on carbonate facies and diagenetic overprint (e.g. dolomitization and karstification). Therefore reservoir characterization on the basis of borehole data (e.g. cuttings, image logs, etc.) and the correlation to seismic data can improve the predictability of the reservoir in areas with sparse or no well data. Most of the geophysical and well data are proprietary and not published, therefore names and exact locations are not given in figures. The seismic data comprises numerous 2D lines, 3D cubes see Figure 3. 18 of the 28 geothermal wells within the AOI or in proximity were used for this study.

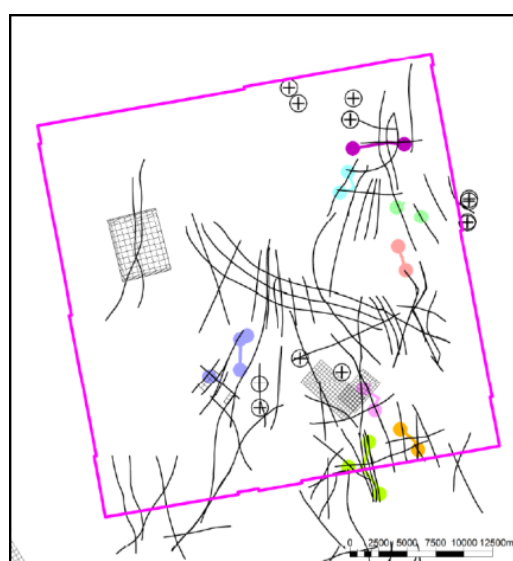


**Figure 3: Model area (pink rectangle) with seismic data 2D (black lines), 3D (black mesh). TD points of geothermal wells are shown as dots with well paths. Wells with the same color belong to the same project. Other geothermal wells with limited data are displayed as black circle with crosses.**

### 3.1 Reservoir Characterisation from Well Data

Reservoir characterisation is done on the basis of cutting material and semi-quantitative thin section analysis. The PDC bits preferably used in the reservoir formation only produce very fine grained cuttings which makes especially the thin section

preparation difficult. Frequently total losses occur in geothermal wells in the AOI, drilling through the partially karstified reservoir. In well sections with total losses no cutting material is available. The information gap is covered by geophysical logs, the most common ones are caliper, gamma-ray, resistivity, sonic and image logs. The last one is particularly of importance for depositional facies interpretation. The description of image log facies is adapted from Steiner and Böhm (2011). Two superior (hyperfacies) and five sub-facies could be classified from the image logs, see Figure 4. For this study only the hyperfacies is of interest, in the AOI nine geothermal wells are available with image log data. Often clearly identifiable as one hyperfacies is the “bedded facies” with thin to medium bedded limestone, marly limestone and minor dolomites. The other hyperfacies is the “mass facies” and is characterized by massive to thick bedded limestone and dolomites.

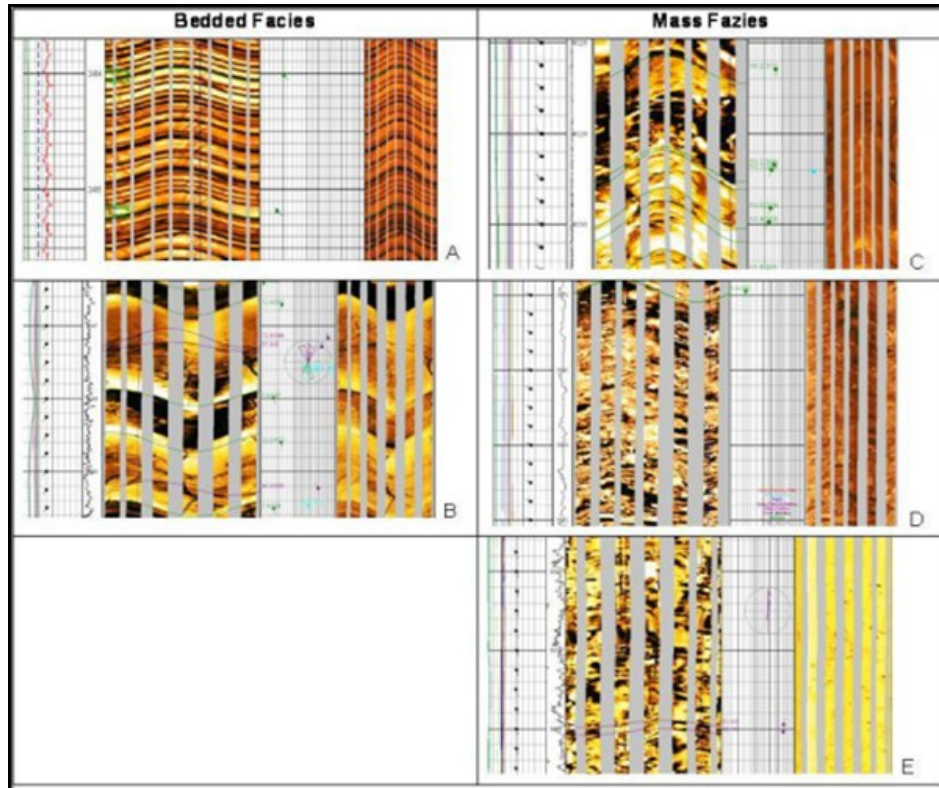


**Figure 4: Interpretation of image log data with two defined hyperfacies Bedded and Mass Facies and five sub-facies (Steiner and Böhm 2011)**

### 3.2 Seismic Interpretation

Seismic reflectors and fault planes were picked on 2D and 3D seismic to establish a seismic stratigraphic framework of the model. Furthermore seismic facies is interpreted within the reservoir horizon from reflection configuration, continuity, amplitude, frequency, interval velocity and external areal association of the seismic facies units, Vail et al. (1977). Sedimentary processes, depositional setting and therefore sedimentary facies (lithology) may be deducted from seismic facies analysis. The differentiation of the Malm reservoir into potential reef-buildups (porous and productive mass facies) and intra-platform basins (tight unproductive bedded/layered facies) is fundamental for hydrothermal exploration in the AOI, Böhm et al. (2013). Additionally seismic attribute analysis may assist in the interpretation of seismic data. The mapping of reflector termination (Figure 5) is an important part of seismic analysis and may yield information about lateral facies changes, depositional environment, (seismic) geobodies and sequence stratigraphic architecture of the reservoir.

### 4. HIGH RESOLUTION GEOCELLULAR FACIES MODEL

Wells (hard data) and seismic (soft data) are not evenly distributed within the AOI (see Figure 3), therefore considerable data gaps occur. To forecast reservoir heterogeneity on an exploration scale and to fill these data and knowledge gaps, a multi scenario geocellular facies model is set up. The general proposed modeling workflow is presented in Figure 6, depending on the knowledge about the reservoir not every step is mandatory. The applied MPS-algorithm (Multiple Point Statistics) has only recently been applied to carbonate systems e.g. Levy et al. (2008), Rankey and Harris (2008), Carrillat et al. (2010), Jung and Aigner (2012) although its application to clastic systems has a longer history e.g. Strebelle and Journel (2001); Strebelle (2002), Harding et al. (2005), Strebelle and Levy (2008).

General proposed MPS modeling workflow:

1. Query the available data and classify potential geobodies after Jung and Aigner (2012).
2. Set up the simulation grid with major hydrostratigraphic units; define the grid cell size appropriate to the input data.
3. Define lateral model zonation e.g. inferred depo-zones.

4. Upscale well data to simulation grid.
5. Create training images for each zone from analogue data implementing depo-elements / -shapes and rules for configuration/interaction of geobodies.
6. Set up deterministic properties e.g. rotation, scaling, affinity and vertical proportion curves.
7. Generate probability models from seismic attributes, -interpretation and other data.
8. Execute simulation with desired number of realizations.
9. QC and revise

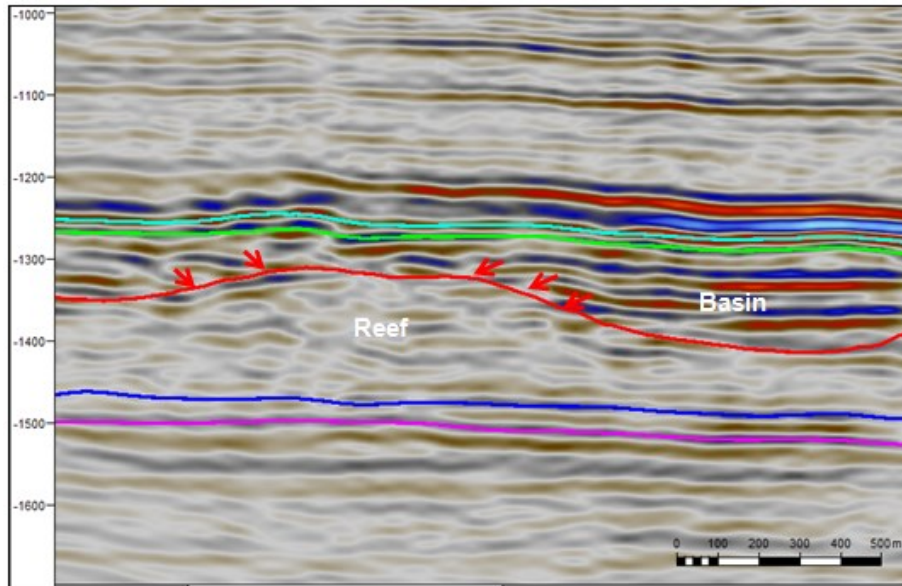


**Figure 5:** Upper seismic section (TWT; 2x exaggerated) with mapped onlaps (red arrows) marking interpreted transition between reefs and intra-platform basins. Horizons: Top Dogger (purple), Base Reservoir (dark blue), Top Reservoir (red), Top Purbeck (green), Top Lithothamnienkalk (light blue).

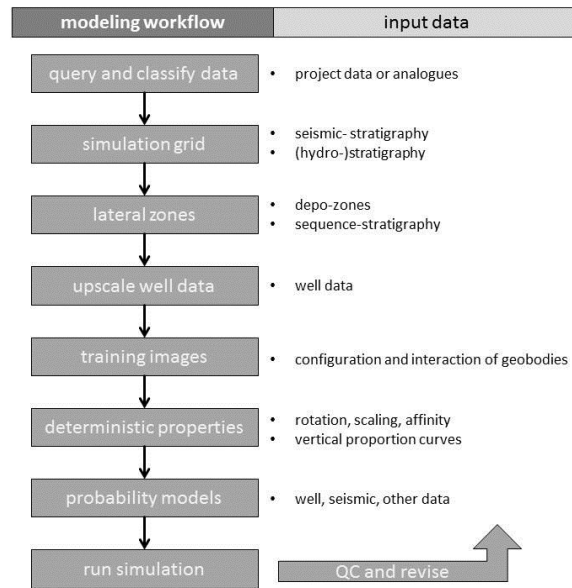


**Figure 6: MPS modeling workflow**

#### 4.1 Query and Classify Data

The lower Malm ( $\alpha$ ,  $\beta$  and  $\gamma$ ) consists dominantly of tight bedded limestone and marls and is therefore considered as hydraulic inactive in the AOI, though there might be early reef development on adjacent paleo-highs e.g. the Landshut reef complex. The

middle Malm ( $\delta$  and  $\epsilon$ ) is considered to be developed most homogenously as dolomitized porous mass-facies interval made from interfingering sponge-algae-oid buildups and sponge-biostromes. This homogenous interval is most important for the large scale hydraulic connectivity of the reservoir and has been observed in all geothermal wells in the AOI. Finally in the upper Malm ( $\xi$ ) the reef- and layered-facies reach their greatest lateral heterogeneity. This interval is due to prolific dolomitization and karstification at the top of the reef-facies a key target for hydrothermal exploration. The reservoir grid of the interval ( $\alpha$  to  $\gamma$ ) and ( $\delta$  to  $\epsilon$ ) are modeled in a deterministic way due to the inferred homogenous facies distribution whereas the heterogeneous facies of the Malm ( $\xi$ ) interval will be modeled with MPS. The Malm ( $\xi$ ) interval is further subdivided into lower, middle and upper Malm ( $\xi$ ).

The Malm ( $\xi$ ) facies may be subdivided in two principal facies types. The first type is the reef-facies also called mass- and bioherm-facies which consists of (often dolomitized) sponge-algae-oid debris or coral-debris. The second type is the layered- or bedded facies representing an intra-platform basin depositional environment, it consists of bedded and layered limestone with abundant index fossils (e.g. ammonites) and interbedded marly layers, Meyer and Schmidt-Kaler (1989).

Dimension, configuration, interrelationship and fractions of depositional facies are derived from the Malm outcrop studies of the southern Franconian Alb, where detailed mapping and outcrop studies are available from manifold authors. However the standard facies maps up to date are those established from Meyer and Schmidt-Kaler (1989), though they give very limited information about facies heterogeneity in the AOI, see Figure 7. For the geocellular facies model it is assumed that the facies patterns and trends derived from the outcrop analogue Franconian Alb sustain also within the AOI. This is however reasonable because the AOI and the Franconian Alb are located on the same vast carbonate platform, also the geothermal wells drilled in the AOI support the idea of small scale facies variations. Paleogeographic maps from Meyer and Schmidt-Kaler (1989) have been georeferenced [GK Zone 4; EPSG: 31468] and depositional facies was mapped in a GIS system comprising maps from the low, middle and upper Malm zeta.

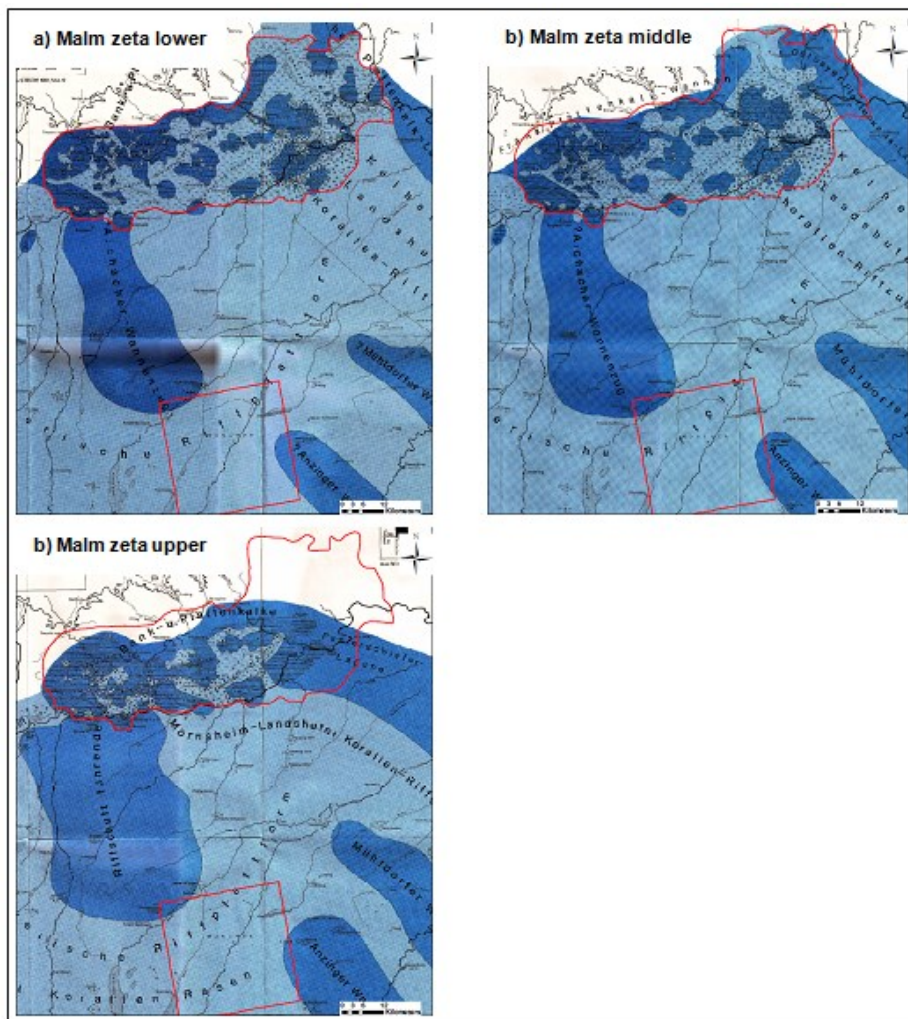


**Figure 7: Paleogeographic maps from Meyer and Schmidt-Kaler (1989) of the lower (a), middle (b) and upper (c) Malm Zeta. The northern (upper) red area encloses the area where the Malm is outcropping (Franconian Alb). The southern (lower) red area encloses the AOI. Layered/bedded facies (dark blue) is interpreted as intra-platform basin facies, mass facies (light blue) is interpreted as reef-core and reef-debris facies.**

#### Summary of orientation/alignment trends from paleogeographic maps

Enclosed intra-platform basins show an orientation of their long axis between 60°-80°, occurring dominantly in the lower and middle Malm zeta. The median dimensions of reef-, reef-flank and intra-platform basin-facies are summarized in Table 1. Isolated

reefs seem to be aligned along the same ENE-WSW trend though slightly shifted to the south (80°-100°). The number and size of isolated reefs increase from the lower to the upper Malm.

**Table 1: Dimensions and configuration of reef and intra-platform basin facies.**

Type	Width [km] Min./Mean/Max ( $\sigma$ )	Length [km] Min./Mean/Max ( $\sigma$ )	Direction [mean]
Reef	0.4/1.7/7.9 (1.8)	0.8/3.0/19.4 (3.5)	ENE-WSW (80-100°)
Intra-platform basin	6.7/4.5/13.9 (3.6)	0.9/7.5/26.5 (6.5)	ENE-WSW (60-80°)

#### 4.2 Upscaling of Well Logs to Simulation Grid

Well data is classified in two hyperfacies mass facies and bedded facies, these are derived from image log data interpretation (see chap. 3.1) and upscaled to the simulation grid. Wells or zones of wells that have no image log data available are classified from cutting analysis and other log data. Mass facies correlates to reef-core facies (F1), bedded facies correlates to intra-platform basin facies (F3), a sequence of interlayered bedded and mass facies correlates to reef-flank facies (F2), see Table 2. The simulation grid cell size was defined as 178x176x1 [m], therefore the Malm ( $\xi$ ) interval comprises 300 layers. The middle Malm ( $\delta$  to  $\epsilon$ ) and the lower interval ( $\alpha$  to  $\gamma$ ) where modeled due to the homogenous facies with only 10 layers each.

**Table 2: Basic data of geobodies**

Code	Geobody type	Image log facies	Depo facies	Depo element	Depo shape	Depo zone
F1	Reef-core	Mass facies	sponge-algae-oooid-coral debris	Core	mound	Open-platform
F2	Reef-flank	Interlayered bedded and mass facies	sponge-algae-oooid-coral debris	Flank	mound	Open- and Protected platform
F3	Intra-platform basin	Bedded facies	layered limestone	sheet	bowl	Protected-platform
F4	Open platform	Bedded facies	marls	background	background	Open-platform

#### 4.3 Training Images

Training images are simplified geological models on a geocellular basis. They display the inferred geological-continuity of geobodies and work as a 3-dimensional semivariogram the MPS algorithm relies on. Three training images were generated, with object modeling incorporating the data from outcrop analysis (see chap. 4.1) to capture the distinctive features of the Malm zeta lower, middle and upper interval. A training-grid of 200x200x100 cells proved to be sufficient, see figure Figure 8.

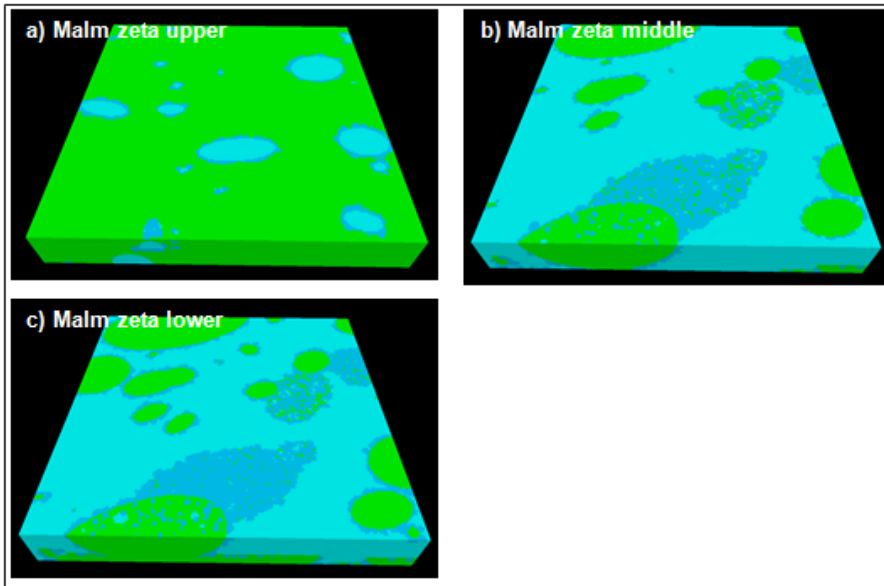


**Figure 8: Training images of the upper (a), middle (b) and lower (c) Malm zeta interval. Intra-platform basin (green), reef-core (light blue), reef-flank (dark-blue).**

Facies proportions used for the training images are summarized in Table 3, which rely on the mapped facies proportion data from paleogeographic map, see Figure 7. The classification of geobody types after Jung and Aigner (2012) that were modeled within the

training image are referred to in Table 1. The reef facies is classified as mound depo-shape and subdivided into two depositional elements reef-core (F1) and reef-flank (F2). The layered facies representing enclosed intra-platform basin facies (F3) is classified as bowl shape build from sheet elements, bedded facies representing open shelf environment is classified as background facies (F4).

#### 4.4 Vertical Proportion Curves

Proportions of reefal and intra-platform basin facies were taken from georeferenced paleogeographic maps Meyer and Schmidt-Kaler (1989). The vertical facies proportions are kept constant over the individual intervals see Table 3, however the MPS algorithm will also honour the input data during the simulation and will therefore scatter around the given values see Figure 9.

**Table 3: Vertical proportion values**

Stratigraphy	Stratigraphic Thickness Mean [m]	Reef (core)	Reef (flank)	Intra-platform basin	Open platform
Malm $\xi$ 3 (upper)	100	7	21	72	0
Malm $\xi$ 2 (middle)	100	26	25	49	0
Malm $\xi$ 1 (lower)	100	43	14	43	0
Malm $(\delta, \varepsilon)$	150	100	0	0	0
Malm $(\alpha, \beta, \gamma)$	75	0	0	0	100

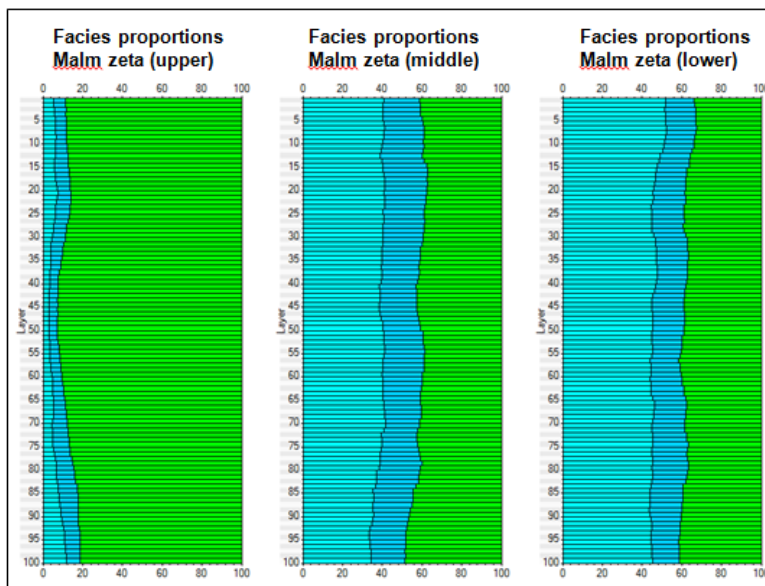


**Figure 9: Vertical proportion curves of a single realization in 300 layers. Reef-core (bright blue), reef-debris (dark blue), intra-platform basin (green)**

#### 4.5 Simulation

Three scenarios with different input data were simulated with MPS and are discussed in regards to facies probability and uncertainty in chap. 5.

##### 4.5.1 Scenario One

For the first simulation only the upscaled well logs (Figure 10) and the training images (Figure 8) are used as input data. This model approach may give the greatest “freedom” to the modeling algorithm. This is particularly visible in the upper Malm zeta where the algorithm matches largely the pattern of the training image. This scenario is most likely the most robust, because only “hard” well data is used. But it also results in considerable facies variability in areas away from the well data, because there is no additional soft data to steer the simulation.

##### 4.5.2 Scenario Two

In this scenario additional to the upscaled wells a probability map is used as input, see Figure 11 (a). Whereas the upscaled well logs are “hard” data and are matched 100% by the MPS algorithm, the probability map is treated as “soft” data and the weight given to the data can be adjusted from 1 to 0, in this scenario a medium range of 0.5 was chosen. The probability map shows the normalized gross thickness of the reservoir, which is derived from seismic mapping. Warm colors of the probability map indicate high probability and cold colors indicate low probability of reef-core facies to occur. A bulge or depression in superimposed strata may occur due to differential compaction of mass-facies and bedded-facies, Heymann (1984). This may result in a measurable difference of total reservoir thickness and the assumption that high reservoir gross thickness indicates a reef body, whereas low gross thickness indicates an intra-platform basin. The interpretation of the gross reservoir thickness is a very robust interpretation, even when the available seismic data is of minor quality.

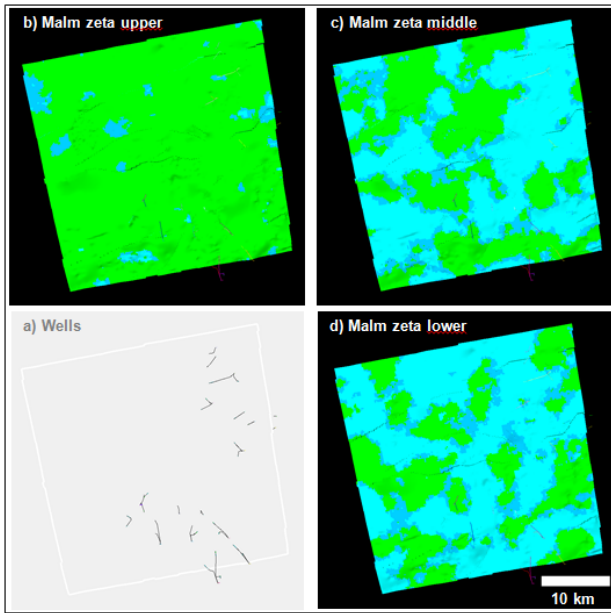


**Figure 10:** Top view of wells used as input data (a). Top view of the three zones modeled with MPS (b-d), intra-platform basin (green), reef-core (light blue), reef-flank (dark-blue).

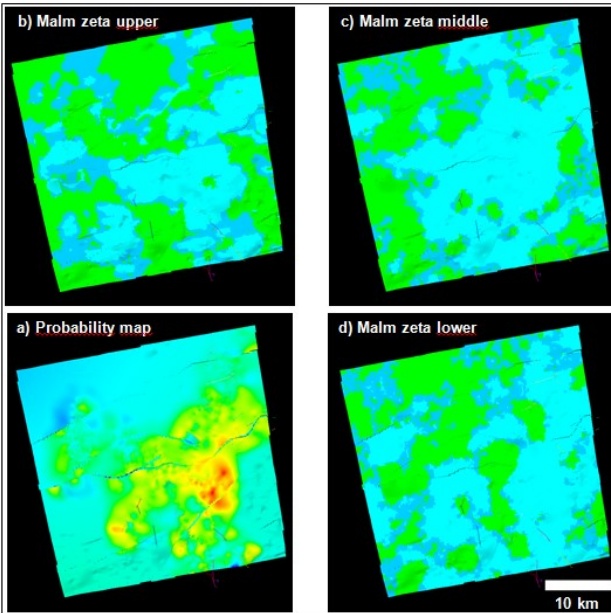


**Figure 11:** (a) Top view of wells and probability map (normalized gross thickness of reservoir) used as input data. Warm colors of the probability map indicate high probability and cold colors indicate low probability of reef-core facies to occur. (b-d) Top view of the three zones modeled with MPS, intra-platform basin (green), reef-core (light blue), reef-flank (dark-blue).

#### 4.5.3 Scenario Three

In this last scenario the probability map indicates the normalized net thickness of the reservoir (Top Reservoir – Base Reservoir), as interpreted from seismic data shown in Figure 5. Warm colors of the probability map indicate high probability and cold colors indicate low probability of reef-core facies to occur. The goodness of the interpretation of the net reservoir thickness is largely dependent on the quality of seismic data. But on the other hand this scenario may reflect best the underlying reservoir trends in the AOI.

#### 5. DISCUSSION FACIES PROBABILITY AND UNCERTAINTY

The three models yield different results of facies distribution, due to different input data (probability maps). The models are superimposed to compare the results of the facies modeling. The probability (or likelihood) of facies occurring in all three models are displayed in Figure 13, showing the top of the three Malm zeta intervals. Warm colors indicate a higher probability of present

reef-core and reef-flank facies, colder colors indicate a higher probability of present intra-platform basin facies within the three models.

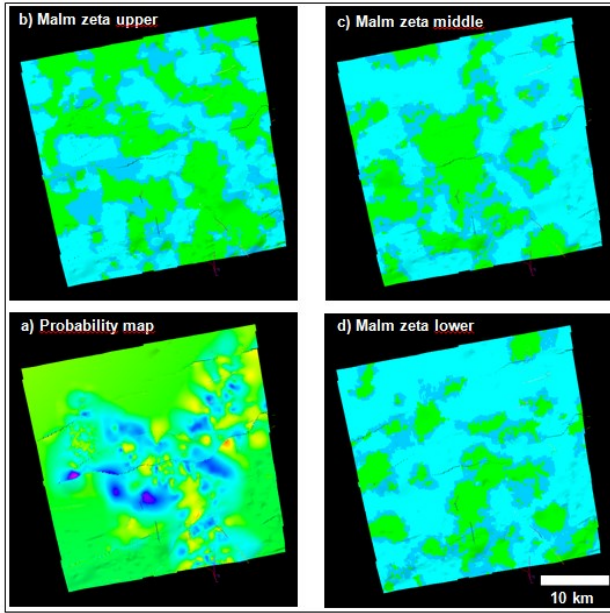


**Figure 12:** (a) Top view of wells and probability map (normalized net thickness of reservoir) used as input data. Warm colors of the probability map indicate high probability and cold colors indicate low probability of reef-core facies to occur. (b-d) Top view of the three zones modeled with MPS, intra-platform basin (green), reef-core (light blue), reef-flank (dark-blue).

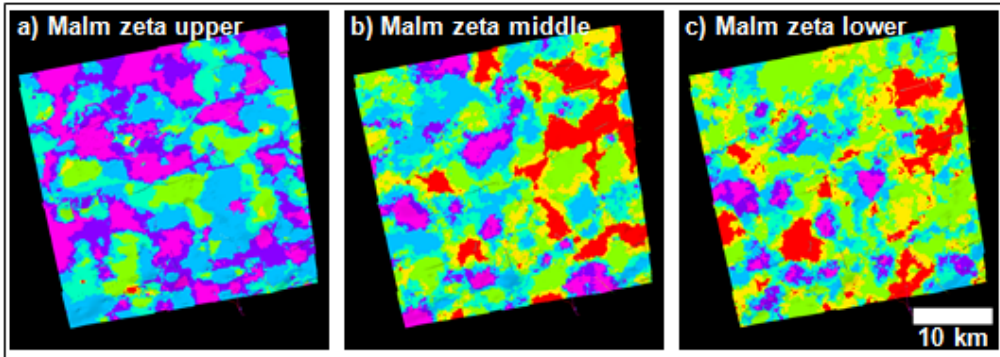


**Figure 13:** Top view of the superimposed models, from upper, middle and lower Malm zeta (a-c). Warm colors indicate a high probability for reef-core-/flank and cold colors indicate high probability of intra-platform basin facies to occur.

The simulation was run ten times for model scenario 3, see chap. 4.5.3. A probability cube for the occurrence of reef facies was calculated from these 10 equiprobable realizations, see Figure 14. Warm colors indicate a high probability; cold colors indicate a low probability of reef-core facies to occur. A possible utilization as an optimization tool for well path design is shown in Figure 14 (d), where the reef-core facies probability is sampled along a proposed well path. A cross section through a probability cube after 100 simulation runs is shown in Figure 15. The reef-core probability cube also reflects the likely geometries of the intra-platform basin facies (purple cells) and of the reef-flank facies (bluish cells).

## 6. CONCLUSIONS

The observations made from nearby outcrop analogues helped to establish a realistic basis for facies modeling on exploration scale in the greater area of Munich (AOI). Due to the number of available well data, the area is an ideal starting point to set up a “standard” facies model for the Malm reservoir in the eastern Molasse Basin. The available image log data greatly improved the model and enhanced the vertical resolution. The conducted MPS simulation proved to deliver realistic facies geometries similar to those of the proposed outcrop analogue at the Franconian Alb. A simulation run may produce multiple equiprobable realizations of the facies model, this delivers a statistical basis to assess facies probability (probability cube) in a discrete space of the model area this could be a license field or a proposed well. The developed geostatistical module (workflow) may also be used as an input for flow simulation, to honor the uncertainty of facies distribution within the reservoir with each realization. These modeling tools focus on creating rapidly available realistic reservoir models by incorporating a variety of data sets. The aim is to minimize exploration risks and in the case of a subsequent flow simulation to forecast more (realistic) production scenarios. The proposed

workflow and modeling techniques are highly flexible and can be adapted to diverse carbonate or clastic reservoirs; also the modeling of diagenetic patterns is possible e.g. karst features in carbonate reservoirs.

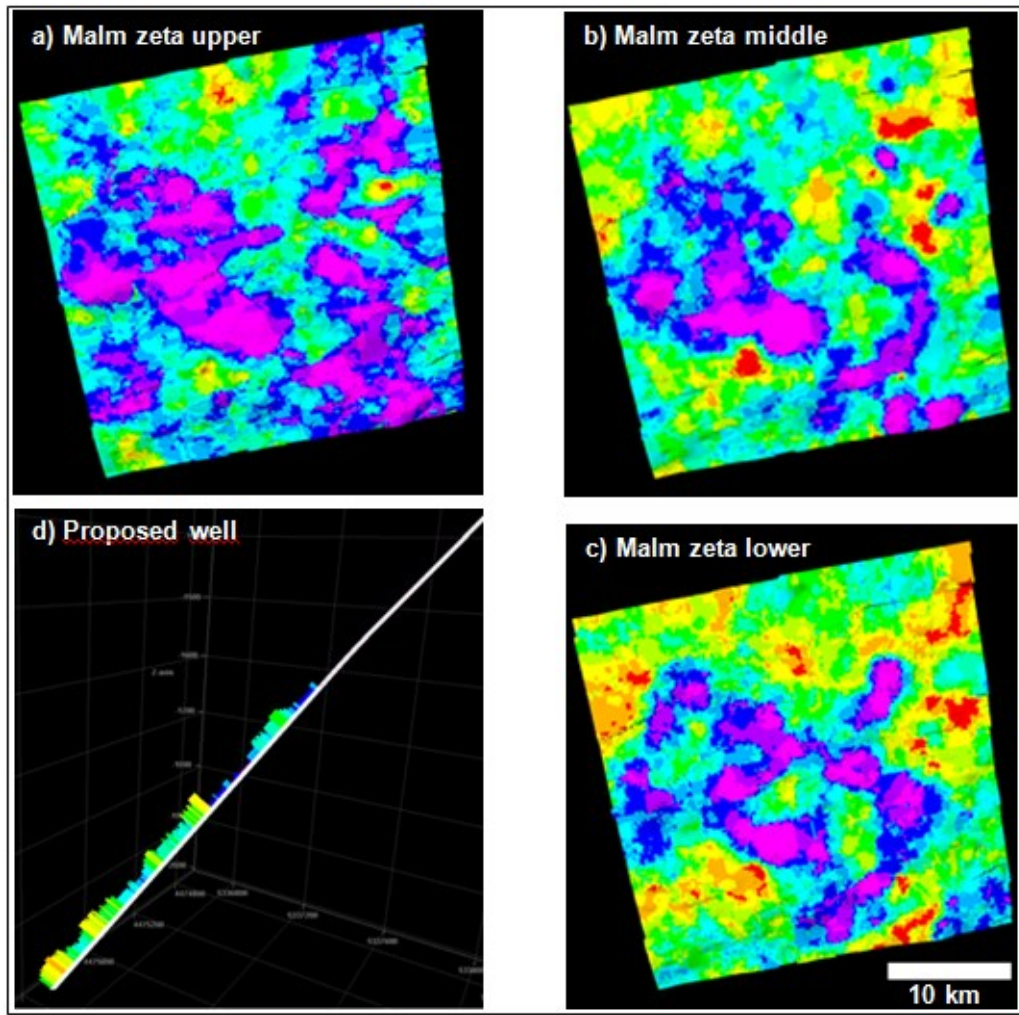


Figure 14: Top view of reef-core facies probability cube (10 realizations), from upper, middle and lower Malm zeta (a-c). Warm colors indicate a high probability (red=1) and cold colors (purple=0) indicate low probability of reef-core facies to occur. (d) Proposed well path with sampled reef-core facies probability.

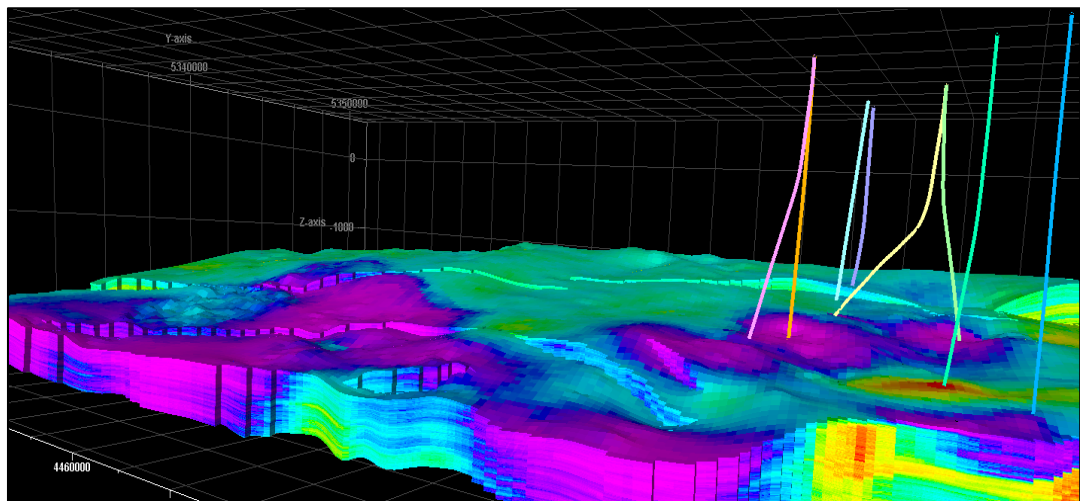


Figure 15: View from the southeast cross-section through the reef-core probability cube (100 realizations) of the upper, middle and lower Malm zeta and selected geothermal wells. Warm colors indicate a high probability (red=1) and cold colors (purple=0) indicate low probability of reef-core facies to occur (3x times vertical exaggerated).

## REFERENCES

Bachmann, G. H., M. Muller, and K. Weggen. 1987. "Evolution of the Molasse Basin (Germany, Switzerland)." *Tectonophysics* 137 (1-4): 77–92.

Böhm, Dipl-Geol Franz, Dipl-Geol Alexandros Savvatis, Dipl-Geol Ulrich Steiner, Prof Dr Michael Schneider, and Prof Dr Roman Koch. 2013. "Lithofazielle Reservoircharakterisierung zur geothermischen Nutzung des Malm im Großraum München." *Grundwasser* 18 (1): 3–13. doi:10.1007/s00767-012-0202-4.

Carrillat, Alexis, Sachin Sharma, Tino Grossmann, Gulanara Iskenova, and Torsten Friedel. 2010. "Geomodeling of Giant Carbonate Oilfields with a New Multipoint Statistics Workflow." In Society of Petroleum Engineers. doi:10.2118/137958-MS. <https://www.onepetro.org/conference-paper/SPE-137958-MS>.

Harding, Andrew, Sebastien Strebelle, Marjorie Levy, Julian Thorne, Deyi Xie, Sebastien Leigh, Rachel Preece, and Robert Scamman. 2005. "Reservoir Facies Modelling: New Advances in MPS." In *Geostatistics Banff 2004*, edited by Oy Leuangthong and Clayton V. Deutsch, 559–68. Quantitative Geology and Geostatistics 14. Springer Netherlands. [http://link.springer.com/chapter/10.1007/978-1-4020-3610-1\\_57](http://link.springer.com/chapter/10.1007/978-1-4020-3610-1_57).

Heymann, H. 1984. "Oberjurassic als Explorationsziel in Bayern". presented at the 6. ÖGEW/DGMK-Gemeinschaftstagung, Innsbruck.

Jung, A., and T. Aigner. 2012. "Carbonate Geobodies: Hierarchical Classification and Database – a New Workflow for 3d Reservoir Modelling." *Journal of Petroleum Geology* 35 (1): 49–65. doi:10.1111/j.1747-5457.2012.00518.x.

Levy, M., P. M.M Harris, S. Strebelle, and E. C Rankey. 2008. "Geomorphology of Carbonate Systems and Reservoir Modeling: Carbonate Training Images, FDM Cubes, and MPS Simulations."

Meyer, R. K.F, and H. Schmidt-Kaler. 1989. *Paläogeographischer Atlas Des Süddeutschen Oberjura (Malm)*. Schweizerbart.

Rankey, EUGENE C., and P. M. Harris. 2008. "Remote Sensing and Comparative Geomorphology of Holocene Carbonate Depositional Systems." *Controls on Carbonate Platform and Reef Development*, 317–22.

Steiner, Ulrich, and Franz Böhm. 2011. "Lithofacies and Structure Signatures of Imagelogs in Carbonates and Their Implications for Reservoir Characterisation in Southern Germany." In Valencia, Spain.

Strebelle, Sebastien. 2002. "Conditional Simulation of Complex Geological Structures Using Multiple-Point Statistics." *Mathematical Geology* 34 (1): 1–21. doi:10.1023/A:1014009426274.

Strebelle, Sebastien, and Andre Journel. 2001. "Reservoir Modeling Using Multiple-Point Statistics." In Society of Petroleum Engineers. doi:10.2118/71324-MS. <https://www.onepetro.org/conference-paper/SPE-71324-MS>.

Strebelle, Sebastien, and Marjorie Levy. 2008. "Using Multiple-Point Statistics to Build Geologically Realistic Reservoir Models: The MPS/FDM Workflow." *Geological Society, London, Special Publications* 309 (1): 67–74. doi:10.1144/SP309.5.

Vail, P. R., R. M. Mitchum Jr, R. G. Todd, J. M. Widmier, S. Thompson III, J. B. Sangree, J. N. Bubb, and W. G. Hatelid. 1977. "Seismic Stratigraphy Applications to Hydrocarbon Exploration." *AAPG Memoir* 26: 49–212.